JOURNAL OF VIROLOGY, Nov. 1997, p. 8592–8601 Vol. 71, No. 11
0022-538X/97/$04.00+0

The Immune System Preferentially Clears Theiler's Virus from the Gray Matter of the Central Nervous System

M. KARIUKI NJENGA,[1,2] KUNIHIKO ASAKURA,[1,2] SAMUEL F. HUNTER,[2] PETER WETTSTEIN,[1] LARRY R. PEASE,[1] AND MOSES RODRIGUEZ[1,2]*

Departments of Immunology[1] and Neurology,[2] Mayo Clinic and Foundation, Rochester, Minnesota 55905

Received 28 May 1997/Accepted 6 August 1997

Infection of susceptible strains of mice with Daniel's (DA) strains of Theiler's murine encephalomyelitis virus (DAV) results in virus persistence in the central nervous system (CNS) white matter and chronic demyelination similar to that observed in multiple sclerosis. We investigated whether persistence is due to the immune system more efficiently clearing DAV from gray than from white matter of the CNS. Severe combined immunodeficient (SCID) and immunocompetent C.B-17 mice were infected with DAV to determine the kinetics, temporal distribution, and tropism of the virus in CNS. In early disease (6 h to 7 days postinfection), DAV replicated with similar kinetics in the brains and spinal cords of SCID and immunocompetent mice and in gray and white matter. DAV RNA was localized within 48 h in CNS cells of all phenotypes, including neurons, oligodendrocytes, astrocytes, and macrophages/microglia. In late disease (13 to 17 days postinfection), SCID mice became moribund and permitted higher DAV replication in both gray and white matter. In contrast, immunocompetent mice cleared virus from the gray matter but showed replication in the white matter of their brains and spinal cords. Reconstitution of SCID mice with nonimmune splenocytes or anti-DAV antibodies after establishment of infection demonstrated that both cellular and humoral immune responses decreased virus from the gray matter; however, the cellular responses were more effective. SCID mice reconstituted with splenocytes depleted of $CD4^+$ or $CD8^+$ T lymphocytes cleared virus from the gray matter but allowed replication in the white matter. These studies demonstrate that both neurons and glia are infected early following DAV infection but that virus persistence in the white matter is due to preferential clearance of virus from the gray matter by the immune system.

Theiler's murine encephalomyelitis viruses (TMEV) are natural enteric pathogens of mice, belonging to the *Picornaviridae* family (51). TMEV strains are divided into two subgroups on the basis of neurovirulence after intracerebral inoculation, GDVII and TO (Theiler's original) subgroups (23, 26, 27). The GDVII subgroup (GDVII and FA strains) produce an acute fatal panencephalomyelitis in mice of all genetic backgrounds (26, 27). Clinically, these mice exhibit flaccid paralysis, circling, and respiratory failure before death. The TO subgroup (Daniel's [DA], BeAn, WW, and Yale strains) produce a biphasic central nervous system (CNS) disease in susceptible strains of mice characterized by acute encephalitis in the first week, followed by a chronic demyelinating disease (23, 39). The demyelinating disease serves as a model of multiple sclerosis in humans. In the chronic phase, TMEV persists in glial cells and macrophages throughout the life of a mouse, resulting in progressive inflammatory myelin destruction in the white matter of the spinal cord (23, 24). Mice with demyelination show clinical signs of paresis, incontinence, spasticity, and paralysis. In resistant strains of mice, the TO subgroup produces a mild acute encephalitis followed by complete clearance of the virus and recovery within 3 weeks (39).

Demyelination occurs only if mice are persistently infected and is due to both direct effects of the virus (45, 46, 54) and immune response of the host (4, 43, 44). Despite extensive studies, the mechanisms of TMEV persistence are not clearly understood. Factors controlling persistence include the genetics of the mouse (6, 36), the genetics of the virus (21, 50, 52, 54), virus cytotropism (3, 11, 20, 34), and immune responses (40). In mice, the *H-2D* allele in the major histocompatibility complex genes (10, 36) and another gene close to the gamma interferon gene locus on chromosome 10 (6) control susceptibility to persistent infection. Some studies have suggested that the GDVII subgroup fails to persist because of lack of genetic determinants of persistence (28, 50), or inability to infect glial cells (26), but other studies have challenged these conclusions (17, 42, 49).

Most studies of TO strains have suggested that a change in tropism from neurons to glial cells, followed by restricted viral RNA and protein synthesis (7, 8, 22), results in persistence of virus in the white matter. This paradigm is based, in part, on ultrastructural studies that demonstrated sequential infection of neurons in the brain, neurons in the spinal cord, and finally glial cells and macrophages in the white matter of the spinal cord, where virus persists and causes chronic demyelination (3, 12, 13, 23). However, detailed in vivo studies to substantiate this sequence of events have not been conducted. In vitro studies have not been useful in resolving the question, because TMEV strains lytically infect neuronal and glial cell cultures with similar kinetics (18, 19, 31). A recent in vivo study indicated that both TO and GDVII viruses infect glia and neurons early, suggesting the possibility that the distinct tissue distribution of virus during persistent infection may not be the result of differential virus tropism (2). We propose that the effective clearance of TO viruses from the gray matter, but not the white matter, by the immune system is the reason for selective persistence in the white matter. To test the hypothesis and detail the pathogenetic sequence of TO virus infection in the CNS, severe combined immunodeficient (SCID) and immunocom-

* Corresponding author. Mailing address: Mayo Clinic, 200 First St. SW, Rochester, MN 55905. Phone: (507) 284-4663. Fax: (507) 284-1637. E-mail: Rodriguez@mayo.edu.

petent C.B-17 mice and SCID mice reconstituted with nonimmune splenocytes or neutralizing antibodies were inoculated intracerebrally with the DA virus (DAV) to determine the kinetics, sequential distribution, tropism, and persistence of the virus. The C.B-17 strain (*H-2*^{d} haplotype) is susceptible to TMEV persistence and demyelination (41).

MATERIALS AND METHODS

Mice. Four- to six-week-old C.B-17 and C.B-17-*scid* (hereafter referred to as SCID) mice (*H-2*^{d} haplotype) were purchased from Taconic Laboratory Animals (Germantown, N.Y.). Mice were inoculated intracerebrally with 2×10^6 PFU of DAV in a 10-μl volume. All mice were bred and maintained in the Mayo Clinic Animal Facility. Handling of all animals conformed to the National Institutes of Health and Mayo Clinic institutional guidelines.

Virus. The DA strain of TMEV was used. The virus was grown in BHK-21 cells and titrated by plaque assay in L2 cells as described previously (38).

Reconstitution of SCID mice. All SCID mice were reconstituted with 3×10^7 splenic cells from BALB/c or C.B-17 mice as described previously (41). This dose of cells was shown previously to protect SCID mice from fatal encephalitis (41). There were two different protocols for reconstitution of SCID mice. In the first protocol, mice were reconstituted by injection of splenocytes intravenously through the tail vein and infected with DAV 3 to 5 h after reconstitution. Some SCID mice were reconstituted with splenocytes depleted of $CD4^+$ or $CD8^+$ T lymphocytes by negative selection with anti-$CD4^+$ (9) or anti-$CD8^+$ (48) antibodies in the presence of complement (41). Based on the estimation that the percentage of $CD3^+$ T lymphocytes in untreated BALB/c or C.B-17 splenocytes was 33%, the numbers of monoclonal antibody- and complement-treated splenocytes were adjusted to ensure that recipients received the same number of T cells of the surviving subpopulation as that received by recipients of untreated splenocytes. Mice reconstituted with CD4-depleted splenocytes also received weekly injections of anti-CD4 GK 1.5 monoclonal antibody (14) to maintain efficient depletion (41). The efficiencies of $CD4^+$ or $CD8^+$ T-lymphocyte depletion in splenocytes were 94.9 and 97.6%, respectively, when the splenocytes were analyzed by flow cytometry (41). In the second protocol, SCID mice were reconstituted with total splenocytes at 3, 7, and 10 days after virus inoculation to examine patterns of virus clearance in different regions of the CNS.

Treatment with anti-DAV antibody. SCID mice were treated with serum harvested from DAV-infected C57BL/6J mice (Jackson Laboratory, Bar Harbor, Maine). The serum had a 50% DAV-neutralizing titer of 1:4,000. SCID mice received 100 μl of serum intraperitoneally twice weekly beginning 3 days after intracerebral DAV inoculation. Mice were sacrificed 17 days after infection and 24 h after the final antibody injection.

Frozen sections. Mice were sacrificed by ether overdosage. The brain was cut into three coronal blocks to allow analysis of the structures of the forebrain, midbrain, and hindbrain. Each brain tissue slide contained three sections from the three regions, enabling detailed analysis of DAV infection in the cortex, corpus callosum, thalamus, hypothalamus, striatum, cerebellum, and brain stem for each animal. The entire spinal cord was cut into three or four blocks to allow analysis of the cervical, thoracic, lumbar, and sacral regions. The spinal cord blocks were then arranged into longitudinal sections such that one tissue slide contained sections from all the blocks, providing a detailed representation of the entire cord. The brain and spinal cord blocks were snap frozen in OCT embedding compound (Miles Inc., Elkhart, Ind.) with isopentane in liquid nitrogen. Sections 10-μm thick were cut with a Reichert-Jung Cryocut 1800 (Cambridge Instruments, Heidelberg, Germany) for immunostaining and in situ hybridization.

Viral plaque assay. Viral plaque assays were performed on brains and spinal cords from immunocompetent and SCID mice as described previously (38). Briefly, brains and spinal cords were collected separately and 10% (wt/vol) homogenates were prepared in Dulbecco modified Eagle medium. The homogenates were sonicated three times for 20 s each and clarified by centrifugation. All dilutions were plated in triplicate. Viral plaques were determined on L2 cells and expressed as $\log_{10}$ PFU per gram of tissue. Virus titers were compared by Student's *t* test.

In situ hybridization. In situ hybridization for DAV RNA was carried out as described previously (29). Briefly, sections fixed in cold phosphate buffer containing 0.5% paraformaldehyde, 0.5% glutaraldehyde, 0.002% calcium chloride, 1.6% glucose, and 1% dimethyl sulfoxide were treated with 1 μg of proteinase K in phosphate-buffered saline for 30 min at 37°C and in 0.1 M triethanolamine containing acetic anhydride for 10 min at room temperature. Slides were prehybridized in buffer containing deionized formamide, Denhardt's solution, sodium chloride, salmon sperm DNA, yeast total RNA, and yeast tRNA for 4 h at room temperature before being hybridized with ^{35}S-labeled 253- or 363-bp cDNA probes corresponding to VP1 of DAV (32). The cDNA probes were obtained by double digestion of the VP1 plasmid with *Kpn*I and *Sal*I restriction enzymes and radiolabeling of the probe with between 0.5×10^8 to 0.8×10^8 cpm of α-^{35}S-dATP per μg of DNA by nick translation. Hybridization was carried out overnight at 37°C followed by extensive washes in reducing buffer at 55°C. Air-dried slides were immersed in NTB2 film emulsion (Eastmann Kodak) and exposed at 4°C for 1 to 3 days.

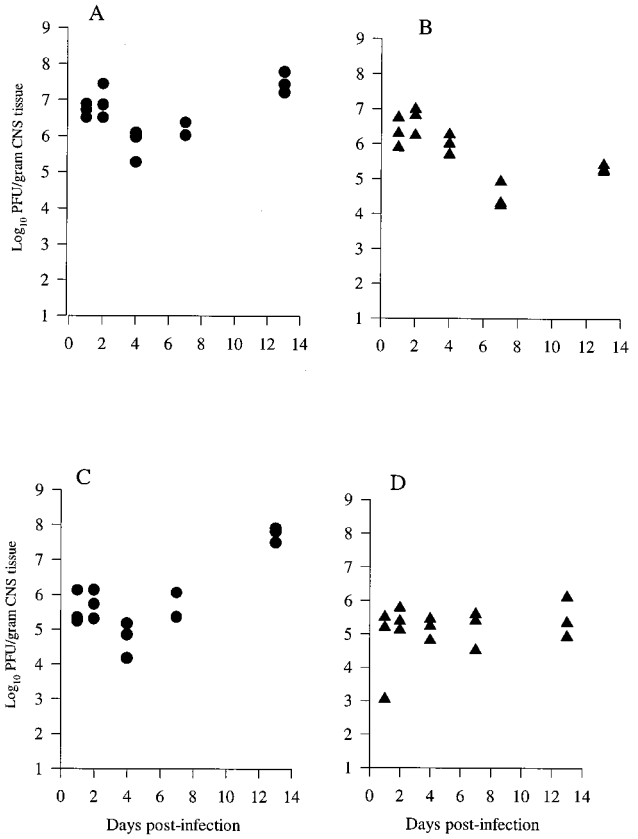

FIG. 1. Virus titers from brains and spinal cords of SCID and immunocompetent C.B-17 mice. (A) SCID mouse brain; (B) C.B-17 mouse brain; (C) SCID mouse spinal cord; (D) C.B-17 mouse spinal cord. Mice were inoculated with 2×10^5 PFU of DAV, and plaque assays were performed on days 1, 2, 4, 7, and 13 p.i. as described previously (38). The limit of detection of this plaque assay was 100 PFU of virus/ml.

DAV RNA-positive cells in various regions of the brain (cerebral cortex, corpus callosum, hippocampus, striatum, hypothalamus, cerebellum, and brain stem) and spinal cord (gray and white matter) were counted by light microscopy at a ×250 magnification. The respective CNS areas (in square millimeters) were measured with the IBAS Image Analysis System (Kontron, Munich, Germany) attached to an Axiophot microscope (Carl Zeiss, Inc., Thornwood, N.Y.) at a ×50 magnification. The data were expressed as the numbers of DAV RNA-positive cells per square millimeter. Statistical comparisons were done by unpaired Student's *t* test.

Immunohistochemical staining for DAV antigens. Brain and spinal cord frozen sections were fixed in cold acetone and incubated with a polyclonal rabbit anti-DAV serum which reacts with capsid proteins of DAV (37). The antigens were detected by the avidin-biotin immunoperoxidase technique.

Simultaneous immunostaining and in situ hybridization. To identify the CNS cells supporting DAV replication, we performed immunocytochemistry using cell markers for oligodendrocytes, astrocytes, macrophages, and neurons followed by in situ hybridization for DAV RNA. We used rabbit antibodies against myelin basic protein (Dako Corp, Santa Barbara, Calif.) for oligodendrocytes, glial fibrillary acidic protein (Dako) for astrocytes, and 200-kDa neurofilaments (Sigma Chemical Co., St. Louis, Mo.) or neuron-specific enolase (Zymed Laboratories, South San Francisco, Calif.) for neurons. *Bandeiraea simplicifolia* BS-1 lectin (Sigma) and anti-Ia antibody (OX-6; Serotec, Oxford, England) were used to identify microglia/macrophages. Following avidin-biotin immunoperoxidase detection, sections were rinsed in distilled water and hybridized in situ for DAV RNA as described above.

Culture and infection of mouse primary glial and neuronal cells. Neuronal cells were obtained from telencephala of newborn BALB/c mice by enzymatic dissociation (53). The cells were seeded on poly-DL-ornithine-coated chamber slides. Neuron cultures contained approximately 55% neurons, 45% type II astrocytes, and less than 1% oligodendrocytes and microglia/macrophages. Primary mixed glial cell cultures were prepared from newborn BALB/c mice as described previously (1). Briefly, whole brains were dissociated, centrifuged, and resuspended in culture medium. The cells were cultured for 10 to 14 days and

TABLE 1. DAV infection in cultured glial and neuronal cells[a]

Cells	No. of cells	No. of DAV-positive cells	% Positive cells	P^b
Mixed glia	235 ± 29	181 ± 32	76 ± 5	
Neurons	190 ± 22	146 ± 18	77 ± 4	0.88

[a] Primary glial or neuronal cells were cultured from neonatal BALB/c mice as described in Materials and Methods. Cultures on chamber slides were infected with DAV at 1 to 5 PFU/cell for 24 h. Slides were washed in phosphate-buffered saline, fixed with cold acetone, and immunostained for DAV antigens by the avidin-biotin immunoperoxidase technique. Cells from 3 to 5 chambers were counted at a ×250 magnification with a light microscope. Data are mean numbers of cells ± standard errors.

[b] Infectivity of neuronal cultures was compared with that of glial cultures by unpaired Students' *t* test.

then seeded onto chamber slides. Glial cell cultures contained approximately 70% astrocytes, 20% microglia/macrophages, and 10% oligodendrocytes. Chamber slides of both cultures were inoculated with 1 to 5 PFU of DAV per cell for 24 h, washed, fixed in cold acetone, and immunostained for viral antigens.

RESULTS

SCID mice have high virus titers and develop signs of acute encephalomyelitis. DAV-infected SCID and immunocompetent C.B-17 mice were observed daily for clinical disease. SCID mice survived for 15 to 17 days and manifested two phases of disease: early disease (6 h to 7 days postinfection [p.i.]), in which mice were clinically normal, and late disease (13 to 17 days p.i.), in which clinical signs of encephalitis were evident without demyelination. In contrast, immunocompetent C.B-17 mice did not show clinical signs of encephalitis but by 45 days p.i. developed persistent DAV infection and chronic demyelination of the spinal cord white matter characterized by mild neurologic signs of spasticity and hind limb paresis.

The kinetics of replication of the virus in the CNS were determined for both SCID and immunocompetent C.B-17 mice. Three mice from each strain were sacrificed at 1, 2, 4, 7, and 13 days p.i., and plaque assays were performed for the brains and spinal cords separately. There was no difference in virus titers at 1 to 4 days p.i. between SCID (Fig. 1A and C) and immunocompetent (Fig. 1B and D) mice ($P > 0.4$). SCID mice had 100- to 1,000-fold more virus than immunocompetent C.B-17 mice at 13 days p.i. ($P = 0.004$). Virus titers were also higher in the brains than in the spinal cords of both SCID ($P = 0.004$) and immunocompetent ($P = 0.0039$) mice when all sacrifice time points were compared.

DAV replicates early in both the gray and the white matter of the brain. We confirmed that DAV can infect both neurons and glial cells in vitro by infecting primary glial (mixed oligodendrocytes, microglia, and astrocytes) and neuronal cultures from neonatal BALB/c ($H\text{-}2^d$ haplotype) mice with DAV and immunostaining for virus antigens (Table 1). BALB/c mice, a strain from which the closely related congenic C.B-17 strain was derived, were used in these experiments. Based on these in vitro results that suggest that virus is inherently competent to infect gray and white matter cells of the CNS, we tested whether DAV replicates equally in neurons and glia in vivo or whether it first replicates in neurons and then switches to glia later as proposed previously (3, 20, 23). SCID and immunocompetent C.B-17 mice were sacrificed 6 and 12 h and 1, 2, 4, 7, 13, and 17 days after infection. Six immunocompetent C.B-17 mice were also sacrificed 45 days after infection (no SCID mice survived to this time point). Frozen brain and spinal cord sections were hybridized in situ with a DAV-specific probe (29), and the distribution of DAV RNA-positive cells in various regions of the CNS was determined. Specificity of the probe was demonstrated in sham (phosphate-buffered saline)-inoculated age-matched SCID mice sacrificed 10 days after inoculation when no hybridization was detected.

DAV replicated equally in gray and white matter of the brains of SCID and immunocompetent mice during the early period (6 h to 7 days p.i.) (Table 2). For example, the numbers of virus-RNA-positive cells in the corpora callosa (white matter) and the pyramidal layers of hippocampi (gray matter) were not statistically different ($P > 0.91$). In SCID mice, virus was detected in the corpora callosa of 11 of 15 mice (73%) and in the pyramidal layers of the hippocampi of 11 of 15 mice (73%)

TABLE 2. DAV-RNA-positive cells in the brains of immunocompetent C.B-17 and SCID mice[a]

Mouse strain	Time p.i.	No. of mice	Mean no. of DAV-RNA-positive cells[b] (range) in:						
			Cortices	Corpora callosa	Hippocampi		Striata	Cerebella	Brain stems
					Pyramidal	Molecular			
SCID	6–24 h	7	0.8 (0–3)	34.2 (0–85)	29.9 (0–100)	3.1 (0–20)	0.3 (0–1)	0.3 (0–2)	0
C.B-17	6–24 h	6	2.5 (0–4.6)	42.3 (0–174)	47.7 (0–173)	4.8 (0–17)	5.3 (1–12)	5.6 (0–9)	0
SCID	48–96 h	4	3.3 (0–10.3)	49.2 (0–166)	>50[d]	8.7 (0.9–19)	3.2 (1–6)	0	0
C.B-17	48–96 h	6	25.3 (0–77)	>50[d]	>50[d]	11 (0–33)	10.4 (2–26)	0.4 (0–2)	0.9 (0–4)
SCID	7 days	5	4.7 (0–15)	11 (0–49)	42.6 (0–152)	4.4 (0–11)	13.3 (1–32)	1.2 (0–6)	0.5 (0–2)
C.B-17	7 days	3	4.2 (3.2–6)	12.3 (0–34)	31.1 (0–75)	3.4 (0–10)	7.7 (6–11)	0.9 (0–3)	0.9 (0–3)
SCID	13 days	4	>50[d]	21.4 (6–120)	>50[d]	>50[d]	17.3 (7–30)	4.5 (0–17)	7.7 (5–10)
C.B-17	13 days	4	0	4.4 (0–10)	0	0	0	0	4.5 (0–13.6)
SCID	15–17 days[c]	6	38.9 (9–60)	16 (6–45)	>50[d]	>50[d]	19.6 (5–44)	3.9 (1–10)	8.4 (2–30)
C.B-17	17 days	10	0	0.9 (0–7)	0	0	0	0	0.7 (0–1.8)
C.B-17	45 days	6	0	0	0	0	0	0	4.5 (0–23)

[a] In situ hybridization with a ^{35}S-labeled probe corresponding to the VP1 region of DAV was carried out on frozen sections of mouse brains and spinal cords. DAV-RNA-positive cells were counted by light microscopy, and the CNS areas were measured with a quantitative image analysis system.

[b] DAV-RNA-positive cells are presented as mean numbers of cells per square millimeter.

[c] SCID mice were moribund 15 to 17 days p.i.; thus, no animals were available for comparison to immunocompetent C.B-17 mice at 45 days p.i.

[d] The positive cells in the different areas of the brain in these sections were too numerous to count.

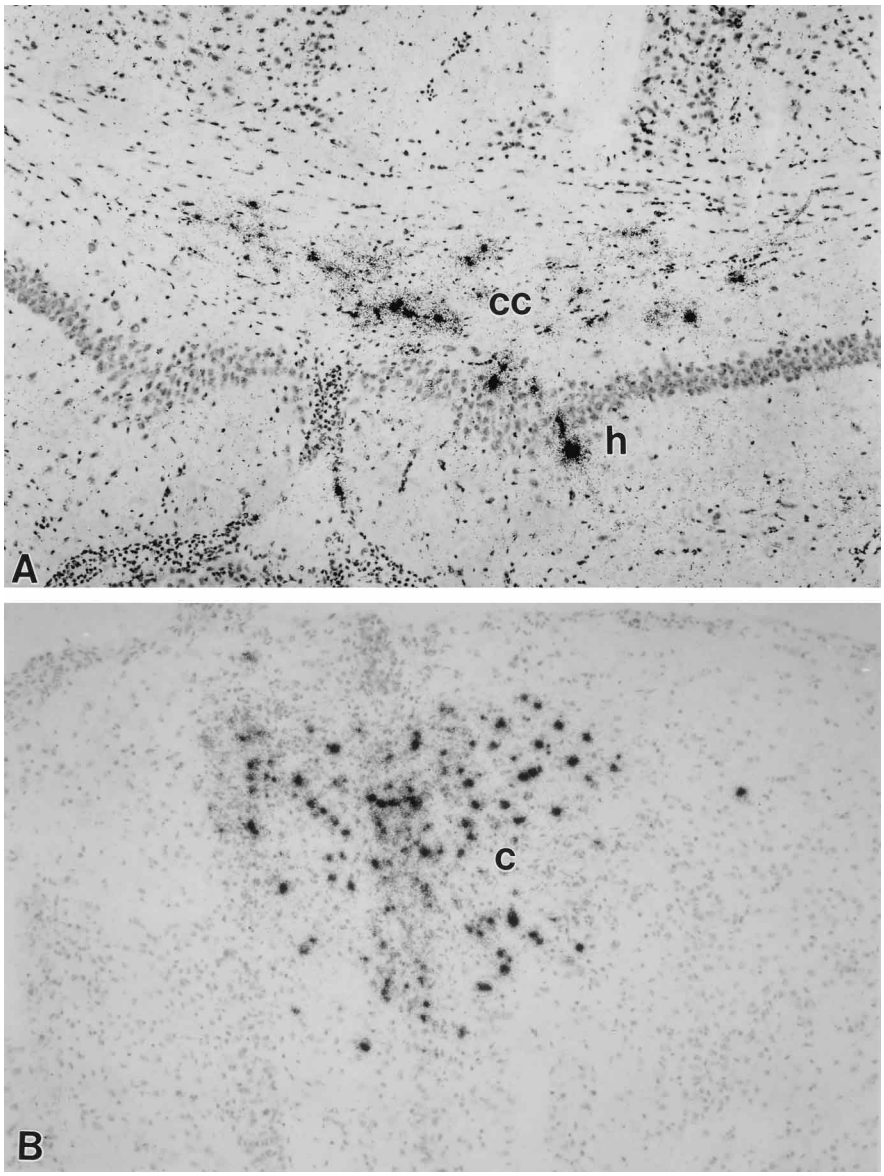

FIG. 2. TMEV replication in both the gray and white matter of the brain in early disease. DAV RNA was localized in frozen sections by hybridization with ^{35}S-labeled probe corresponding to the VP1 region of DAV. Virus replication in the corpus callosum (cc) (white matter) and the hippocampus (h) (gray matter) 24 h p.i. (A) and in the cerebral cortex (c) (gray matter) 4 days p.i. (B) of an immunocompetent mouse is shown. A similar pattern and levels of virus replication were detected in SCID mice 24 h and 4 days after infection. Sections were counterstained lightly with Mayer's hematoxylin. Magnification for both pictures, ×100.

between 6 h and 7 days p.i., whereas in immunocompetent C.B-17 mice, virus was detected in the corpora callosa of 10 of 15 mice (66.7%) and in the pyramidal layers of the hippocampi of 12 of 15 mice (80%). The primary sites of DAV replication in the first 96 h of infection were in the hippocampus and corpus callosum (Fig. 2A), but the virus spread rapidly to the cerebral cortex (Fig. 2B), striatum, and brain stem. Virus replicated in both the left and right horns of the hippocampus and in the corpus callosum, eliminating the possibility that virus localization in those regions was as a result of injection. An exception was the dentate gyrus of the hippocampus and the large Purkinje cells and neurons of the granular layer of the cerebellum, in which virus-positive cells were rarely detected.

In late disease (13 to 17 days p.i.), DAV replicated to high levels in all regions of the brain in SCID mice (Fig. 3A). In contrast, virus was cleared from most of the brains of immunocompetent mice (Fig. 3B), except the white matter of the corpora callosa and brain stems (Table 2). These results confirmed the importance of B and T lymphocytes in virus clearance from the brain and suggested that clearance is more effective in the gray than in the white matter.

Virus replicates in CNS parenchymal cells of all phenotypes during early infection. CNS cells supporting DAV replication in early disease (1 to 7 days p.i.) were identified by simultaneous immunostaining of brain sections for CNS cell phenotypes and hybridizing for DAV RNA. Fidelity of the colocalization technique was confirmed by comparing the distribution of double-positive cells (cell phenotype and virus RNA positive) with that of single-positive cells (viral RNA positive) in serial sections. Typically, immunostaining reduced the sensi-

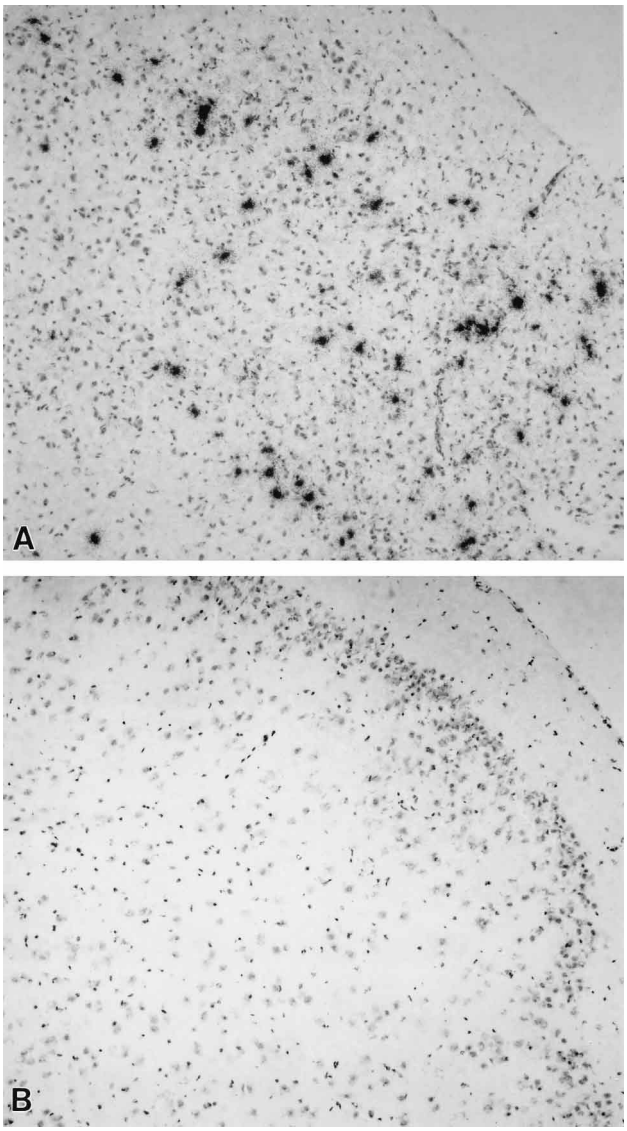

FIG. 3. Clearance of TMEV from the gray matter of immunocompetent, but not SCID, mice 17 days after infection. DAV RNA was localized in frozen sections by hybridization with ^{35}S-labeled probe corresponding to the VP1 region of DAV. Sections of the cerebral cortices of a SCID mouse showing extensive DAV replication (A) and of an immunocompetent mouse which cleared virus (B) are shown. Sections were counterstained lightly with Mayer's hematoxylin. Magnification for both pictures, ×81.

tivity of subsequent in situ hybridization. Even though the numbers of DAV-RNA-positive cells were fewer in the double-labeled than in the single-labeled sections, the distribution patterns were the same. In both SCID and immunocompetent C.B-17 mice, oligodendrocytes (Fig. 4A), astrocytes (Fig. 4B), neurons (Fig. 4C), and macrophages/microglia (Fig. 4D) supported virus replication. Oligodendrocytes and astrocytes positive for DAV were detected in both the gray and the white matter. More neurons and fewer macrophage/microglia supported DAV replication in SCID mice than in immunocompetent C.B-17 mice (Table 3). We concluded that DAV can efficiently infect both neurons and glial cells in early disease.

Preferential clearance of virus from the gray matter of the CNS. The spinal cord is the primary site of TMEV persistence and chronic demyelinating disease. We detected virus-positive cells in the spinal cords of only 2 of 12 immunocompetent C.B-17 mice and in none of 11 SCID mice before day 4 p.i. The virus was detected in cells of both gray and white matter of the spinal cords of all mice at 7 days p.i. (Fig. 5). However, in late disease (13 to 17 days p.i.) virus replication was higher in gray than in white matter in SCID mice (Fig. 5A and 6A) whereas it was predominantly in the white matter in immunocompetent C.B-17 mice (Fig. 5B and 6B). In SCID mice 13 to 17 days p.i., the gray matter showed extensive neuronal necrosis whereas the white matter had normal morphology. In immunocompetent C.B-17 mice 17 and 45 days p.i., the white matter showed extensive inflammatory infiltrates and widespread virus infection whereas neurons in the gray matter appeared morphologically normal. These data indicated that DAV preferentially replicated in the gray matter in the absence of B and T lymphocytes but persisted in the white matter in the presence of a competent immune system.

Both humoral and cellular immune responses are effective in clearing DAV from gray matter. To examine immune-mediated clearance more specifically, we first infected SCID mice with DAV and then at 3 days p.i. reconstituted them with either splenocytes ($n = 5$) or DAV-neutralizing antibodies ($n = 3$). The efficiencies of reconstitution and antibody treatment were confirmed by quantitation of both total immunoglobulin G (>400 μg/ml in splenocyte-reconstituted mice, <10 μg/ml in antibody-treated mice, and <10 ml/μg in unreconstituted SCID mice) and DAV-specific immunoglobulin G (high levels in splenocyte- and anti-DAV antibody-reconstituted mice and none in unreconstituted mice) in serum 17 days p.i. Both the splenocyte-reconstituted and antibody-treated SCID mice were protected from encephalitis and remained clinically normal until they were sacrificed 17 days p.i. In the animals reconstituted with splenocytes 3 days after infection, DAV replication was 2- to 20-fold higher in the white matter than in the gray matter of their spinal cords (Fig. 7), with the exception of the level in one mouse which had similar amounts of virus-positive cells in the gray and white matter. In the animals treated with DAV-neutralizing antibodies, the levels of virus replication were two- to fourfold higher in the white matter than in the gray matter (Fig. 7). These results demonstrated that both a cellular immune response (T lymphocytes) and antibodies can decrease virus from the gray matter but that the humoral response is less effective. SCID mice reconstituted with splenocytes developed severe white matter demyelination.

As a control, SCID mice ($n = 3$) were reconstituted at day 3 p.i. with 3×10^7 splenocytes derived from SCID mice. These mice succumbed to acute encephalitis, with one dying at day 11 p.i. and the other two being sacrificed in a moribund state at day 13 p.i. DAV RNA was localized predominantly in the gray matter (mean of 33.2 virus-positive cells/mm^2), whereas replication levels in the white matter were similar to those observed in reconstituted mice (mean of 6.9 virus-positive cells/mm^2). DAV-infected mice reconstituted at 7 ($n = 5$) and 10 ($n = 5$) days p.i. developed severe encephalitis and died 11 to 13 days p.i. associated with high virus replication in the gray matter (mean of 52 virus-positive cells/mm^2). The levels of virus replication in the white matter of these late reconstituted mice were similar to those observed in early reconstituted mice (mean of 10.1 virus-positive cell/mm^2) (Fig. 7).

Either CD4- or CD8-depleted splenocytes are effective in clearing DAV from gray matter. To determine whether T-lymphocyte subpopulations are critical for clearing DAV from gray matter, we reconstituted SCID mice with total splenocytes, CD4-depleted splenocytes, or CD8-depleted splenocytes and injected them with DAV intracerebrally 3 to 5 h later. Mice were sacrificed 17 to 21 days p.i., and the distribution of

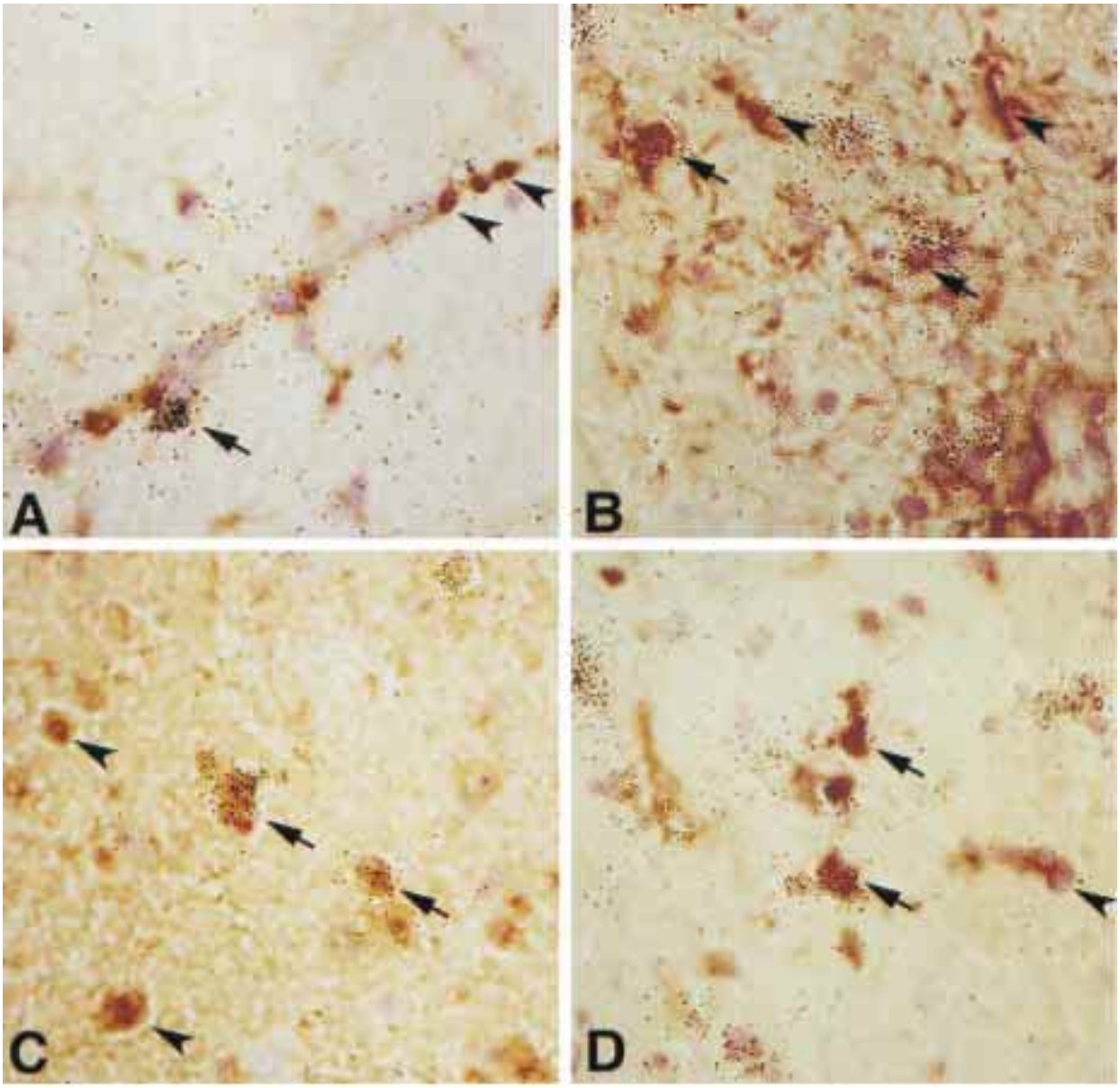

FIG. 4. Colocalization of DAV RNA in cell phenotypes in SCID and immunocompetent mice in early disease (4 to 7 days p.i.). CNS cells were identified by immunostaining of brain sections with anti-myelin basic protein for oligodendrocytes (A), anti-glial fibrillary acidic protein for astrocytes (B), anti-neuron-specific enolase for neurons (C), and *B. simplicifolia* BS-1 lectin for microglia/macrophages (D). Immediately after immunostaining, slides were hybridized with ^{35}S-labeled probe for DAV. Brown-stained cells containing grains (arrows) are positive for the cell type and DAV RNA. Some cells were positive for cell markers but negative for virus (arrowheads). Slides were counterstained lightly with Mayer's hematoxylin. Magnification for all pictures, ×3,400.

the virus in the spinal cord white and gray matter was analyzed. In SCID mice reconstituted with total splenocytes, DAV replication was detected exclusively in the white matter (mean of 7.5 virus-positive cells/mm^2) but not in the gray matter (Fig. 6C and 8). In mice reconstituted with CD4-depleted or CD8-depleted splenocytes, virus was effectively cleared from the gray matter (<1 virus-positive cell/mm^2) but replicated in the white matter to levels similar to those in mice reconstituted with total splenocytes (means of 6.5 and 11.1 virus-positive/mm^2 for CD4- and CD8-depleted mice, respectively) (Fig. 8). These data demonstrated that neither CD4$^+$ nor CD8$^+$ T lymphocytes are individually required to effectively clear DAV from the gray matter of the CNS, in agreement with the findings with class II major histocompatibility complex- or β_2-

TABLE 3. CNS cells supporting DAV replication in early disease[a]

Mouse strain	No. of cells counted	No. of mice	MBP-positive cells (%)	GFAP-positive cells (%)	NF-positive cells (%)	Ia-positive cells (%)
SCID	195	5	24.6	29.7	38.5	7.2
C.B-17	306	5	28.4	26.1	22.2	23.2

[a] Phenotype-specific antigens for CNS cells and DAV RNA were colocalized by simultaneous immunostaining and in situ hybridization of frozen coronal brain sections from mice infected with DAV for 4 to 7 days. We used the following antibodies: anti-myelin basic protein (MBP) for oligodendrocytes, anti-glial fibrillary acidic protein (GFAP) for astrocytes, antineurofilament (NF) for neurons, and anti-Ia for macrophages/microglia. A ^{35}S-labeled VP1 probe was used to hybridize viral RNA. Cells positive for the cell marker (brown) and DAV RNA (black grains) were counted at a 250× oil objective with a light microscope.

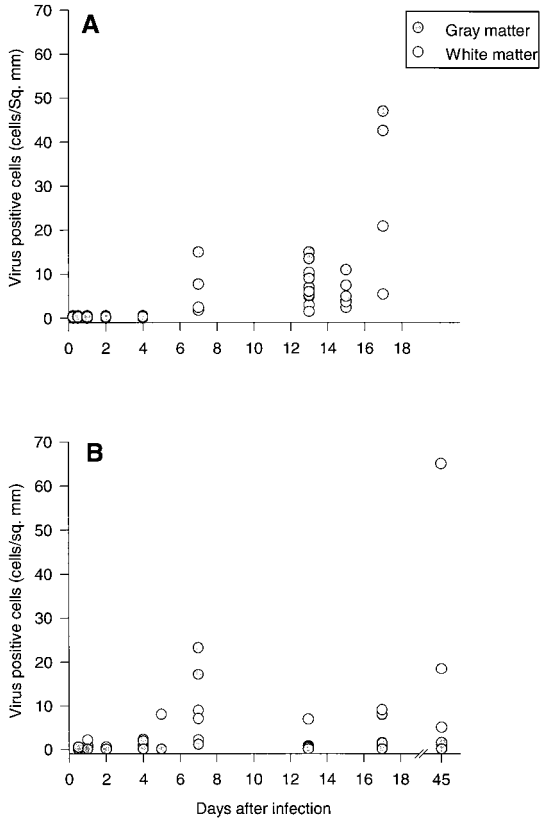

FIG. 5. More effective clearance of DAV from the gray matter than the white matter by the immune system. The sequential distribution of DAV in the spinal cords of SCID and immunocompetent mice following intracerebral inoculation was analyzed with sections hybridized with ^{35}S-labeled VP1 probe. DAV RNA-positive cells were counted with a light microscope, and the area of white or gray matter was measured with an image analysis system. DAV-RNA-positive cells are presented as cells per square millimeter. Distributions in SCID mice indicating predominant virus replication in the gray matter in late disease (A) and in immunocompetent mice indicating predominant virus replication in the white matter in late disease (B) are shown. In early disease, virus replication increased in gray matter, peaking at 7 days p.i. in both strains.

microglobulin-deficient mice which lack functional $CD4^+$ (16, 30) or $CD8^+$ (15, 33, 35) T lymphocytes, respectively. SCID mice reconstituted with either CD4-depleted or CD8-depleted splenocytes developed severe white matter demyelination.

Selective persistence is not the result of emergence of DAV mutants with a predilection for the white matter. One possible reason for the failure of the immune system to clear virus from the white matter in late disease is that immunologic pressure causes the emergence of DAV mutants specific for the white matter. To test this hypothesis, we isolated DAV from the spinal cords of immunocompetent C.B-17 mice infected for 21 days (virus is predominantly in the white matter at this stage) and infected SCID mice with the white matter isolate. Spinal cords were homogenized, sonicated, and clarified by centrifugation before plaque assay to titrate the virus. Ten SCID mice were infected with this DAV isolated from the spinal cords without in vitro passaging (at a dose of 2.4×10^2 PFU in a 30-μl volume), and five mice were sacrificed at 7 and 17 days p.i. The virus replicated in both the white and gray matter in the brains and spinal cords of the SCID mice (data not shown), indicating that there was no immunologic selection of viral mutants in the CNS.

DAV persists predominantly in oligodendrocytes and astrocytes in the spinal cord white matter. There is controversy on the types of CNS cells that support TMEV replication during chronic demyelination. Some studies have reported that TMEV persists predominantly in oligodendrocytes and astrocytes (3, 30), whereas others found viral antigen mostly in macrophages (25, 47). To address this issue, we colocalized antigens to identify cell phenotypes and DAV RNA in spinal cord sections of demyelinated immunocompetent C.B-17 mice 45 days p.i. DAV RNA was localized in 65% of myelin basic protein-positive cells (oligodendrocytes), 25.6% of glial fibrillary acidic protein-positive cells (astrocytes), and 9.3% of Ia-positive cells (microglia/macrophages) but not in neurons.

DISCUSSION

A paradigm for the change in virus cytotropism based on the sequential distribution of virus replication in the CNS has been proposed previously (3, 5, 20, 23). This hypothesis attributes TMEV persistence in the white matter to changed tropism (from neurons to glial cells) accompanied by restricted viral replication in the glial cells. However, in vitro (18, 19, 31) and in vivo (7, 8, 54) studies have not supported such differential tropisms in neurons and glia. For example, TMEV consistently infects both neurons and glial cells with similar kinetics in vitro (18). In addition, no differences in tropism have been observed when a variant strain of TMEV that caused diminished late disease was compared with the wild-type demyelinating TMEV (54). In the present study, the first detailed analysis of the sequential distribution and tropism of TMEV in the early 6-to-96-h p.i. stage, we found that DAV replicated in gray and white matter to equal levels before the onset of critical virus-specific immune responses. The kinetics of virus replication were similar in early disease in SCID and immunocompetent mice. Moreover, we observed similar levels of virus replication in CNS cells of all phenotypes as early as 6 h after infection. These findings demonstrate conclusively that DAV infects glia early and argue against differential tropisms as the cause of persistence in the white matter in susceptible strains of mice. The results are in agreement with the results of a study (2) that demonstrated early infection of glial cells by DAV but differ from results of earlier ultrastructural studies (3, 12, 13, 23) that demonstrated virus predominantly in neurons in early disease. The reason for the differences can be attributed to the fact that some of the earlier studies (3, 12, 23) analyzed virus distribution from day 7 p.i., at which time TMEV is predominantly in the gray matter in the brain (Table 2), whereas others (3, 13) analyzed the spinal cord, but not the brain, which is the site of inoculation and, therefore, early virus replication.

We propose that the host immune system, which plays a major part in TMEV-induced myelin destruction (4, 43, 44), is more effective in clearing virus from the gray matter than the white matter of the CNS. Although SCID mice replicated DAV in both gray and white matter, virus was predominantly in the gray matter of the brains and spinal cords in late disease (13 to 17 days p.i.). In contrast, immunocompetent mice replicated virus in both gray and white matter in early disease but almost exclusively in the white matter in late disease. In addition, virus was cleared from most parts of the brain except the white matter tracts of the brain stem. This result indicated that in the absence of B and T lymphocytes, DAV preferentially replicated in the gray matter but that the immune cells cleared virus more effectively from gray than white matter. The reconstitution experiments confirmed that both cellular and humoral immune responses can decrease DAV levels in the gray matter but that T lymphocytes are critical in clearing the infection.

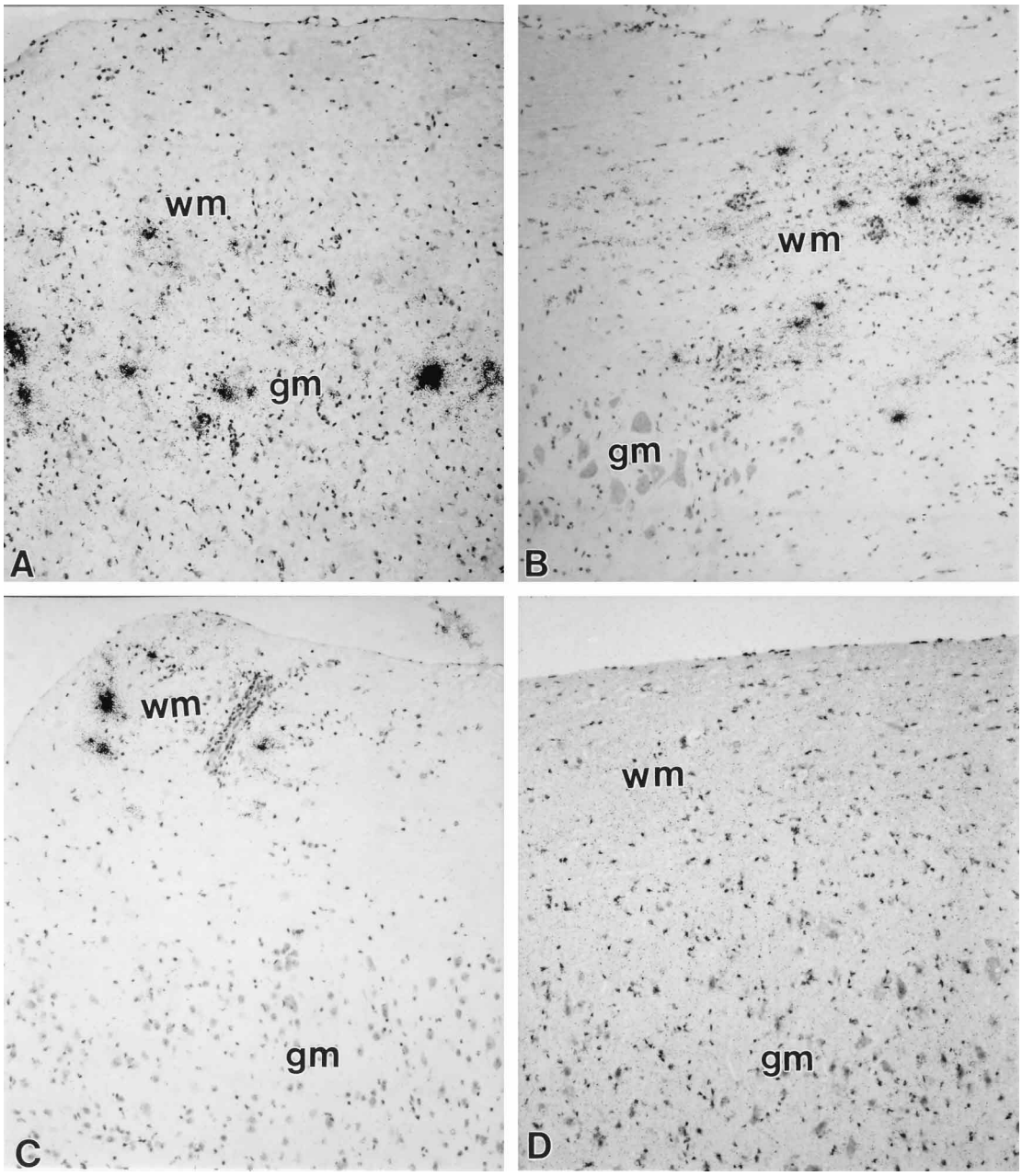

FIG. 6. Selective DAV replication in the white matter of immunocompetent and spleen cell-reconstituted SCID mice as compared to that in SCID mice. Spinal cord sections were hybridized with ^{35}S-labeled probe for DAV. (A) SCID mouse infected for 17 days showing virus predominantly in the gray matter and not in the white matter; (B) immunocompetent C.B-17 mouse infected for 17 days indicating virus predominantly in the white matter; (C) SCID mouse reconstituted with splenocytes 3 to 5 h before DAV inoculation and sacrificed 17 days later, showing virus replication exclusively in the white matter; (D) SCID mouse inoculated with phosphate-buffered saline (17 days) showing absence of DAV RNA-positive cells in the spinal cord. wm, white matter; gm, gray matter. Slides were counterstained lightly with Mayer's hematoxylin. Magnification for all four pictures, ×100).

Neither $CD4^+$ nor $CD8^+$ T-lymphocyte subsets were individually required for clearance of virus from the gray matter, in agreement with findings from knockout mice lacking functional $CD4^+$ (16, 30) or $CD8^+$ (15, 33, 35) T lymphocytes.

The mechanism by which B and T lymphocytes preferentially clear virus from the gray matter, thus allowing persistence in the white matter, is not clear. Preferential clearance may be a function of differences in the anatomies of the gray and white matter of the spinal cord (i.e., vasculature and access of inflammatory cells to different regions of the CNS), or it may be an evolutionary strategy to protect the irreplaceable gray matter neurons in the CNS. The finding that both DAV-neutralizing antibodies and lymphocytes can independently decrease DAV in the gray matter indicates that the mechanism for the preferential clearance applies to both humoral (antibodies) and cellular immune responses. The fact that TMEV-induced demyelination is characterized by extensive infiltration of inflammatory cells associated with foci of virus-positive cells (39) suggests a sustained but unsuccessful attempt by the immune system to clear virus-infected cells from the white matter. Fac-

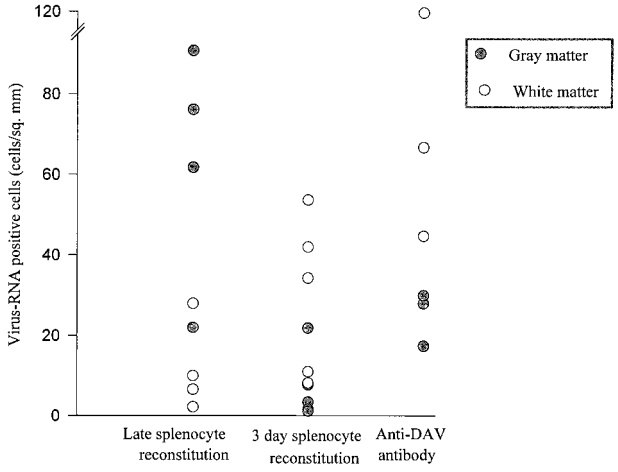

FIG. 7. Preferential clearance of DAV from the gray matter in SCID mice reconstituted following virus infection. Distribution of DAV was analyzed in the spinal cord gray and white matter of SCID mice reconstituted with splenocytes or anti-DAV antibodies 3 days after infection. DAV-RNA-positive cells were counted with a light microscope, and the areas of white or gray matter were measured with an image analysis system. SCID mice reconstituted with splenocytes at days 7 and 10 p.i. succumbed to acute encephalitis, becoming moribund 11 to 13 days p.i. ($n = 4$) (late reconstitution), and replicated virus predominantly in their gray matter. In contrast, splenocyte-reconstituted ($n = 5$) or anti-DAV antibody-treated ($n = 3$) mice 3 days p.i. showed virus primarily in their white matter.

tors such as restricted virus replication (7, 8) and ineffective viral antigen presentation by glial cells may play roles in rendering TMEV clearance ineffective in the white matter. For example, B10 ($H\text{-}2^b$-haplotype) mice are resistant to DAV infection, clearing virus within 3 weeks. However, virus persistence in the white matter occurs when total body irradiation is administered prior to TMEV inoculation (40). More importantly, even after the immune system has fully recovered from irradiation (by day 45 p.i.), these mice are unable to clear virus from the spinal cord white matter (40), suggesting that alteration in virus replication in glial cells causes infected cells to evade clearance.

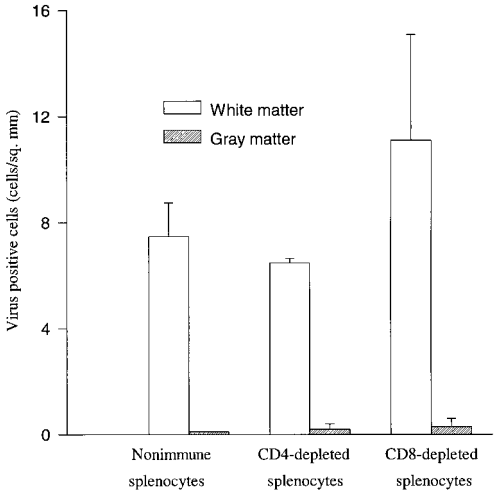

FIG. 8. Levels of virus replication in the gray and white matter of the spinal cords of SCID mice reconstituted with nonimmune splenocytes or splenocytes depleted with anti-CD4 or anti-CD8 antibodies in the presence of complement. Mice were reconstituted 3 to 5 h before intracerebral virus inoculation and sacrificed 17 to 21 days later. Spinal cord sections were immunostained for DAV antigens by an immunoperoxidase technique or hybridized in situ with a ^{35}S-labeled VP1 probe for DAV. Virus-positive cells were counted by light microscopy (magnification, ×25), and the areas of white and gray matter were measured with an image analysis system. Data are means ± standard errors of the means.

In the absence of the immune system, TMEV replicated predominantly in the gray matter in late disease. One possible mechanism of the selective persistence in the white matter of immunocompetent mice is that immunologic pressure causes the emergence of TMEV mutants with a predilection for the white matter. We tested this hypothesis by infecting SCID mice with DAV recovered directly from the spinal cords of immunocompetent C.B-17 mice (no in vitro passage). The DAV isolated from the spinal cords of these mice replicated in both gray and white matter in the brains and spinal cords of SCID mice. Therefore, there does not appear to be immune-mediated selection of viral mutants with a predilection for the white matter.

We also examined the CNS cell phenotypes supporting TMEV persistence within the spinal cord white matter during chronic demyelinating disease. A controversy on the types of cells supporting TMEV replication during persistent infection exists. Some studies (7, 8, 22, 34, 37) found virus persistence primarily in oligodendrocytes and astrocytes, whereas others (11, 25, 47) found TMEV predominantly in macrophages/microglia. Persistence of virus in oligodendrocytes suggested that TMEV directly injures the myelin-producing cells to cause primary demyelination. The direct viral cytolysis hypothesis is supported by ultrastructural studies that localized TMEV antigens within the inner and outer oligodendroglial loops which connect directly with myelin sheaths (34, 37). Other studies found virus persistence predominantly in macrophages, suggesting a nonspecific bystander mechanism in myelin destruction (11, 25). Myelin damage, according to the bystander hypothesis, is caused by cytokines and phagocytic cells recruited to the infection site. In the present study, DAV persisted predominantly in oligodendrocytes, and to a lesser extent in astrocytes and macrophages, but not neurons. The discrepancy in results of the studies examining cells supporting TMEV replication during persistence may be due to differences in virus strains and the genetics of the host. Studies using the DAV and BeAn strains of TMEV are under way in our laboratory to address this issue.

In conclusion, this study indicates a pathogenetic sequence following intracerebral inoculation with a TO strain of TMEV in susceptible mice that begins with the virus infecting both the gray (neurons) and white (glial cells) matter equally in the brain. Subsequently, the virus is cleared by the immune system from most of the brain, except the white matter tracts. In the spinal cord, the virus infects the gray and white matter but is completely cleared from the gray but not the white matter. In the absence of the immune system, the virus replicates more in the gray matter than in the white matter of the spinal cord. In this paradigm, demyelination may be the consequence of a sustained attempt by the immune system to clear DAV from the white matter of the spinal cord.

ACKNOWLEDGMENTS

This work was supported by the National Institutes of Health grants NO1-AI-4-5197, RO1 NS24180, and RO1 NS32129. M. Kariuki Njenga is supported by National Institutes of Health postdoctoral fellowship 1 F32 NS10290-01.

We thank Laurie Zoecklein, Loc Nguyen, Kevin Pavelko, and Maya Shreiber for technical assistance and Julian Leibowitz for helpful discussions and a review of the manuscript.

REFERENCES

1. **Asakura, K., D. J. Miller, K. Murray, R. Bansal, S. E. Pfeiffer, and M. Rodriguez.** 1996. Monoclonal autoantibody SCH94.03, which promotes central nervous system remyelination, recognizes an antigen on the surface of oligodendrocytes. J. Neurosci. Res. **43:**273–281.
2. **Aubert, C., and M. Brahic.** 1995. Early infection of the central nervous system by the GDVII and DA strains of Theiler's virus. J. Virol. **69:**3197–3200.
3. **Aubert, C., M. Chamorro, and M. Brahic.** 1987. Identification of Theiler's virus infected cells in the central nervous system of mouse during demyelinating disease. Microb. Pathog. **3:**319–326.
4. **Borrow, P., P. Tonks, C. R. Welsh, and A. A. Nash.** 1992. The role of CD8+ T cells in the acute and chronic phases of Theiler's murine encephalomyelitis virus-induced disease in mice. J. Gen. Virol. **1992:**1861–1865.
5. **Brahic, M., W. G. Stroop, and J. R. Baringer.** 1981. Theiler's virus persists in glial cells during demyelinating disease. Cell **26:**123–128.
6. **Bureau, J.-F., X. Montagutelli, F. Bihl, S. Lefebvre, J.-L. Guénet, and M. Brahic.** 1993. Mapping loci influencing the persistence of Theiler's virus in the murine central nervous system. Nat. Genet. **5:**87–91.
7. **Cash, E., M. Chamorro, and M. Brahic.** 1985. Theiler's virus RNA and protein synthesis in the central nervous system of demyelinating mice. Virology **144:**290–294.
8. **Cash, E., M. Chamorro, and M. Brahic.** 1986. Quantitation, with a new assay, of Theiler's virus capsid protein in the central nervous system of mice. J. Virol. **60:**558–563.
9. **Ceredig, R., J. W. Lowenthal, M. Nabholz, and H. R. MacDonald.** 1985. Expression of interleukin-2 receptor as a differentiation marker on intrathymic stem cells. Nature **314:**98–100.
10. **Clatch, R. J., R. W. Melvold, S. D. Miller, and H. L. Lipton.** 1985. Theiler's murine encephalomyelitis virus (TMEV)-induced demyelinating disease in mice is influenced by the H-2D region: correlation with TMEV-specific delayed-type hypersensitivity. J. Immunol. **135:**1408–1414.
11. **Clatch, R. J., S. D. Miller, R. Metzner, M. C. Dal Canto, and H. L. Lipton.** 1990. Monocytes/macrophages isolated from the mouse central nervous system contain infectious Theiler's murine encephalomyelitis virus (TMEV). Virology **176:**244–254.
12. **Dal Canto, M. C., and H. L. Lipton.** 1975. Primary demyelination in Theiler's virus infection: an ultrastructural study. Lab. Invest. **33:**626–637.
13. **Dal Canto, M. C., and H. L. Lipton.** 1982. Ultrastructural immunohistochemical localization of virus in acute and chronic demyelinating Theiler's virus infection. Am. J. Pathol. **106:**20–29.
14. **Dialynas, D. P., D. B. Wilde, P. Marrack, A. Pierres, K. A. Wall, W. Havran, G. Otten, M. R. Loken, M. Pierres, J. Kappler, and F. W. Fitch.** 1983. Characterization of murine antigenic determinant, designated L3T4a recognized by monoclonal antibody GK 1.5: expression of L3T4a by functional T cell clones appears to correlate primarily with class II MHC antigen reactivity. Immunol. Rev. **74:**29–56.
15. **Fiette, L., C. Aubert, M. Brahic, and C. P. Rossi.** 1993. Theiler's virus infection of β_2-microglobulin-deficient mice. J. Virol. **67:**589–592.
16. **Fiette, L., M. Brahic, and C. Rossi-Penna.** 1996. Infection of class II-deficient mice by DA strain of Theiler's virus. J. Virol. **70:**4811–4815.
17. **Fu, J., M. Rodriguez, and R. P. Roos.** 1990. Strains from both Theiler's virus subgroups encode a determinant for demyelination. J. Virol. **64:**6345–6348.
18. **Graves, M. C., L. Bologa, L. Siegel, and H. Londe.** 1986. Theiler's virus in brain cell cultures: lysis of neurons and oligodendrocytes and persistence in astrocytes and macrophages. J. Neurosci. Res. **15:**491–501.
19. **Graves, M. C., H. Londe, J. Merril, A. Verity, and R. Nishimura.** 1984. Theiler's virus infection of cultured oligodendrocytes. Ann. Neurol. **16:**151. (Abstract.)
20. **Jarousse, N., L. Fiette, R. A. Grant, J. M. Hogle, A. McAllister, T. Michiels, C. Aubert, F. Tangy, M. Brahic, and C. P. Rossi.** 1994. Chimeric Theiler's virus with altered tropism for the central nervous system. J. Virol. **68:**2781–2786.
21. **Jarousse, N., R. A. Grant, J. M. Hogle, L. Zhang, A. Senkowski, R. P. Roos, T. Michiels, M. Brahic, and A. McAllister.** 1994. A single amino acid change determines persistence of a chimeric Theiler's virus. J. Virol. **68:**3364–3368.
22. **Levy, M., C. Aubert, and M. Brahic.** 1992. Theiler's virus replication in brain macrophages cultured in vitro. J. Virol. **66:**3188–3193.
23. **Lipton, H. L.** 1975. Theiler's virus infection in mice: an unusual biphasic disease process leading to demyelination. Infect. Immun. **11:**1147–1155.
24. **Lipton, H. L., J. Kratochvil, P. Seth, and M. C. Dal Canto.** 1984. Theiler's virus antigen detected in mouse spinal cord 2 1/2 years after infection. Neurology **34:**1117–1119.
25. **Lipton, H. L., G. Twaddle, and M. L. Jelachich.** 1995. The predominant virus antigen burden is present in macrophages in Theiler's murine encephalomyelitis virus-induced demyelinating disease. J. Virol. **69:**2525–2533.
26. **Liu, C., J. Collins, and E. Sharp.** 1967. The pathogenesis of Theiler's GDVII encephalomyelitis virus infection in mice as studied by immunofluorescent technique and infecting titration. J. Immunol. **98:**46–55.
27. **Lorch, Y., A. Friedmann, H. L. Lipton, and M. Kotler.** 1981. Theiler's murine encephalomyelitis virus group includes two distinct genetic subgroups that differ pathologically and biologically. J. Virol. **40:**560–567.
28. **McAllister, A., F. Tangy, C. Aubert, and M. Brahic.** 1990. Genetic mapping of the ability of Theiler's virus to persist and demyelinate. J. Virol. **64:**4252–4257.
29. **Miller, D. J., C. Rivera-Quinones, M. K. Njenga, J. L. Leibowitz, and M. Rodriguez.** 1995. Spontaneous central nervous system remyelination in β2 microglobulin deficient mice following virus-induced demyelination. J. Neurosci. **15:**8345–8352.
30. **Njenga, M. K., K. D. Pavelko, J. Baisch, L. Xiaoqi, C. David, J. Leibowitz, and M. Rodriguez.** 1996. Theiler's virus persistence and demyelination in major histocompatibility complex class II-deficient mice. J. Virol. **70:**1729–1737.
31. **Ohara, Y., H. Konno, Y. Iwasaki, T. Yamamoto, H. Terunuma, and H. Suzuki.** 1990. Cytotropism of Theiler's murine encephalomyelitis viruses in oligodendrocyte-enriched cultures. Arch. Virol. **114:**293–298.
32. **Ohara, Y., S. Stern, J. Fu, L. Stillman, L. Klaman, and R. P. Roos.** 1988. Molecular cloning and sequence determination of DA strain of Theiler's murine encephalomyelitis virus. Virology **164:**245–255.
33. **Pullen, L. C., S. D. Miller, M. C. Dal Canto, and B. S. Kim.** 1993. Class I deficient resistant mice intracerebrally inoculated with Theiler's virus show an increased T cell response to viral antigens and susceptibility to demyelination. Eur. J. Immunol. **23:**2287–2293.
34. **Rodriguez, M.** 1985. Virus induced demyelination in mice: "dying back" of oligodendrocytes. Mayo Clin. Proc. **60:**433–438.
35. **Rodriguez, M., A. J. Dunkel, R. L. Thiemann, J. Leibowitz, M. Zijlstra, and R. Jaesnisch.** 1993. Abrogation of resistance to Theiler's virus-induced demyelination in H-2b mice deficient in beta 2-microglobulin. J. Immunol. **151:**266–276.
36. **Rodriguez, M., J. Leibowitz, and C. S. David.** 1986. Susceptibility to Theiler's virus-induced demyelination: mapping of the gene within the H-2D region. J. Exp. Med. **163:**620–631.
37. **Rodriguez, M., J. L. Leibowitz, and P. W. Lampert.** 1983. Persistent infection of oligodendrocytes in Theiler's virus-induced encephalomyelitis. Ann. Neurol. **13:**426–433.
38. **Rodriguez, M., J. L. Leibowitz, H. C. Powell, and P. W. Lampert.** 1983. Neonatal infection with the Daniel's strain of Theiler's murine encephalomyelitis virus. Lab. Invest. **49:**672–678.
39. **Rodriguez, M., E. Oleszak, and J. Leibowitz.** 1987. Theiler's murine encephalomyelitis: a model of demyelination and persistence of virus. Crit. Rev. Immunol. **7:**325–366.
40. **Rodriguez, M., A. K. Patick, and L. R. Pease.** 1990. Abrogation of resistance to Theiler's virus-induced demyelination in C57BL mice by total body irradiation. J. Neuroimmunol. **26:**189–199.
41. **Rodriguez, M., K. D. Pavelko, M. K. Njenga, W. C. Logan, and P. J. Wettstein.** 1996. The balance between persistent virus infection and immune cells determines demyelination. J. Immunol. **157:**5699–5709.
42. **Rodriguez, M., and R. P. Roos.** 1992. Pathogenesis of early and late disease in mice infected with Theiler's virus, using intratypic recombinant GDVII/DA viruses. J. Virol. **66:**217–225.
43. **Rodriguez, M., and S. Sriram.** 1988. Successful therapy of Theiler's virus-induced demyelination (DA strain) with monoclonal anti-lyt-2 antibody. J. Immunol. **140:**2950–2955.
44. **Roos, R. P., S. Firestone, R. Wollmann, D. Variakojis, and B. G. W. Arnason.** 1982. The effects of short term and chronic immunosuppression on Theiler's virus demyelination. J. Neuroimmunol. **2:**223–234.
45. **Roos, R. P., and R. Wollmann.** 1984. DA strain of Theiler's murine encephalomyelitis virus induces demyelination in nude mice. Ann. Neurol. **15:**494–499.
46. **Rosenthal, A., R. S. Fujinami, and P. W. Lampert.** 1986. Mechanism of Theiler's virus-induced demyelination in nude mice. Lab. Invest. **54:**515–522.
47. **Rossi, C. P., M. Delcroix, I. Huitinga, A. McAllister, N. van Rooijen, E. Claasen, and M. Brahic.** 1997. Role of macrophages during Theiler's virus infection. J. Virol. **71:**3336–3340.
48. **Sarmiento, M., A. L. Glasebrook, and F. W. Fitch.** 1980. IgG or IgM monoclonal antibodies reactive with different determinants on the molecular complex bearing Lyt 2 antigen block T cell-mediated cytolysis in the absence of complement. J. Immunol. **125:**2665–2672.
49. **Simas, J. P., H. Dyson, and J. K. Fazakerley.** 1995. The neurovirulent strain of Theiler's virus can replicate in glial cells. J. Virol. **69:**5599–5606.
50. **Tangy, F., M. McAllister, C. Aubert, and M. Brahic.** 1991. Determinants of persistence and demyelination of the DA strain of Theiler's virus are found only in the VP1 gene. J. Virol. **65:**1616–1618.
51. **Theiler, M.** 1934. Spontaneous encephalitis of mice—a new virus disease. Science **80:**122–123.
52. **Wada, Y., M. L. Pierce, and R. S. Fujinami.** 1994. Importance of amino acid 101 within capsid protein VP1 for modulation of Theiler's virus-induced disease. J. Virol. **68:**1219–1223.
53. **Weber, A., and M. Schachner.** 1984. Maintenance of immunocytologically identified purkinje cells from mouse cerebellum in monolayer culture. Brain Res. **311:**119–130.
54. **Zurbriggen, A., M. Yamada, C. Thomas, and R. S. Fujinami.** 1991. Restricted virus replication in the spinal cords of nude mice infected with Theiler's virus variants. J. Virol. **65:**1023–1030.